Raman spectroscopy of single-domain multiferroic $BiFeO_3$

R. Palai,[1] H. Schmid,[2] J. F. Scott,[3] and R. S. Katiyar[1]
[1]*Department of Physics and Institute for Functional Nanomaterials, University of Puerto Rico, San Juan, Puerto Rico 00931, USA*
[2]*Department of Inorganic, Analytical and Applied Chemistry, University of Geneva, CH-1211 Geneva 4, Switzerland*
[3]*Department of Physics, Cavendish Laboratory, University of Cambridge, Cambridge CB3 0HE, United Kingdom*
(Received 14 November 2007; revised manuscript received 7 February 2010; published 23 February 2010)

We report the investigation of polarized Raman spectroscopy of multiferroic bismuth ferrite ($BiFeO_3$) from 81–273 K, using a ferroelectric/ferroelastic single-domain crystal with an as-grown pseudocubic (pc) $(100)_{pc}$-oriented surface, compared with $(001)_{pc}$ thin film, grown by pulsed laser deposition. The polarized Raman spectra of the single crystal taken at different crystallographic orientations agree with the rhombohedral crystal structure with C_{3v} point group, whereas the $(001)_{pc}$ thin film shows monoclinic structure, contrary to the bulklike rhombohedral and tetragonal structures reported earlier, but consistent with the recent synchrotron radiation studies. Earlier Raman scattering measurements on single crystals violated theoretical predictions. This may be due to mechanical polishing, which allows forbidden *E* (LO) scattering [J. F. Scott, J. Chem. Phys. **48**, 874 (1968); **49**, 98 (1968)]. All of the different phonon vibrations (A_1 and *E* modes) in the single crystal have unambiguously been assigned.

DOI: 10.1103/PhysRevB.81.064110 PACS number(s): 78.30.−j, 68.55.−a, 63.20.−e, 68.49.Uv

I. INTRODUCTION

$BiFeO_3$ (BFO) has been hailed as an important multiferroic material for magnetoelectric devices. Understanding of its symmetry is very crucial for device applications. The symmetry of BFO in thin-film form has been controversial: there have been several probably incorrect reports claiming tetragonal[1,2] or rhombohedral crystal class,[3–5] until synchrotron studies showed definitively monoclinic[6] structure of (001) BFO films on $SrTiO_3$ (STO) substrates. There are several reports[7–15] on Raman scattering measurements on *polished* single crystals but there is no agreement on phonon vibrations and none of them satisfies Raman selection rules. Our aim in the present work is to examine an as-grown single-domain single crystal to exclude the effect of mechanical polishing and an epitaxial thin film to test the synchrotron x-ray results spectroscopically, and to compare with good single-domain single-crystal results. Since conventional x-ray diffraction (XRD) is not very sensitive to detect the crystal structure of thin films, giving uncertain positioning of the oxygen ions, we used micro-Raman spectroscopy to explore the structural insights of the epitaxial thin films and single-domain single crystal.

II. EXPERIMENTAL DETAILS

The growth of our dendritic BFO single crystals with pseudocubic (pc) $(100)_{pc}$ facets and exhibiting both a ferroelectric and ferroelastic as-grown single-domain state is described in Ref. 16.

BFO thin films of 300 nm thickness were grown by pulsed laser deposition (PLD) using a 248 nm KrF Lambda Physik laser. Films were grown on STO(100) substrates of area $(5\ mm)^2$ with a ~25-nm-thick $SrRuO_3$ (SRO) bottom electrode. The orientation of the films was examined using a Siemens D5000 X-ray diffractometer. The Jobin Yvon T64000 micro-Raman microprobe system with Ar ion laser ($\lambda = 514.5$ nm) in backscattering geometry was used for polarized and temperature-dependant Raman scattering. The laser excitation power was 2.5 mW and the acquisition time was 10 min per spectrum.

III. RESULTS AND DISCUSSION

A. Brief review on $BiFeO_3$ single-crystal Raman studies

In the present section we will briefly review polarized Raman scattering measurements on $BiFeO_3$ single crystal. $BiFeO_3$ crystallizes in a distorted perovskite structure, rhombohedral with space group $R3c$. The rhombohedral structure can be represented as a cubic $Pm\bar{3}m$ structure by antiphase tilt of the adjacent FeO_6 octahedra ($\bar{a}\ \bar{a}\ \bar{a}$ in Glazer's notation[17]) and a displacement of both the Fe^{3+} and Bi^{3+} cations from their centrosymmetric position along the pseudocubic $[111]_{pc}$ direction. The rhombohedral ($R3c$), tetragonal ($P4mm$),[1] and monoclinic (Bb) (Ref. 18) structures of BFO give rise to 13, 8, and 27 distinct Raman-active modes, respectively

$$\Gamma_{Rhombohedral,\ R3c(C_{3v})} = 4A_1 + 9E, \tag{1}$$

$$\Gamma_{Tetragonal,\ P4mm(C_{4v})} = 3A_1 + B_1 + 4E, \tag{2}$$

$$\Gamma_{Monoclinic,\ Bb(C_s)} = 13A' + 14A''. \tag{3}$$

The Raman selection rules for the different crystal classes are given in Table I in Ref. 19. Bulk BFO has a rhombohedral crystal structure up to 820 °C with space group $R3c(C_{3v})$. According to the Raman selection rules (provided *Z* is the polar axis of the trigonal system) in $Z(XX)\bar{Z}$ scattering configuration there should be only 13 Raman active modes (four A_1 modes and nine *E* modes). Whereas there will be only nine *E* modes in $Z(XY)\bar{Z}$ and $Y(ZX)\bar{Y}$ scattering directions. Although the BFO single crystal has been studied by several groups[7–12] for better understanding of the phonon modes, none of the reports has reported the observa-

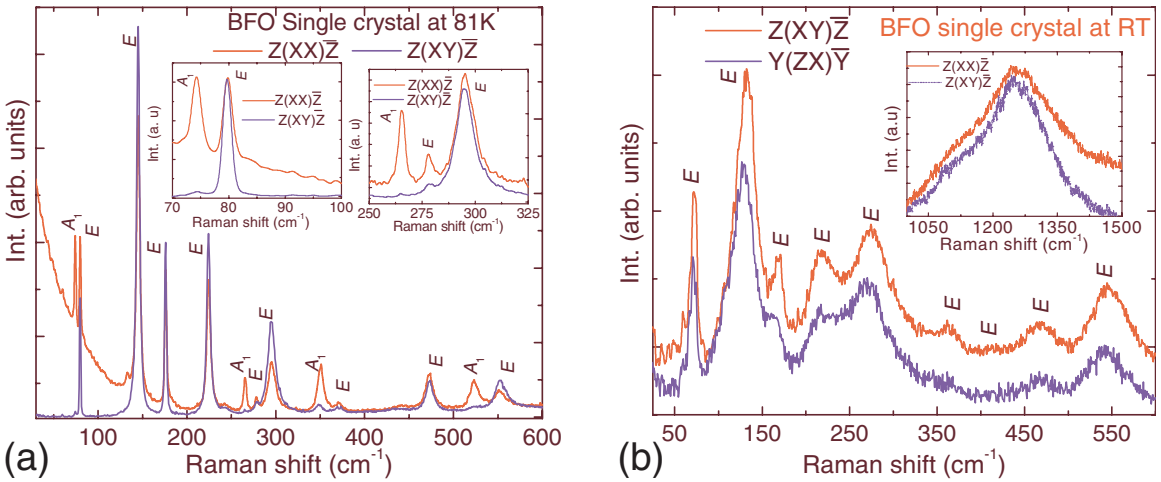

FIG. 1. (Color online) Polarized Raman spectra of single-domain $BiFeO_3$ single crystal; (a) scattering along $Z(XX)\bar{Z}$ and $Z(XY)\bar{Z}$ polarization configurations at 81 K. The insets show magnification of 70–100 wave numbers and 250–325 wave numbers; (b) along $Z(XY)\bar{Z}$ and $Y(ZX)\bar{Y}$ configurations at room temperature. Inset shows a multiphonon peak observed at ~1250 cm^{-1} in $Z(XX)\bar{Z}$ and $Z(XY)\bar{Z}$ configurations.

tion of 13 and 9 Raman modes in $Z(XX)\bar{Z}$ and $Z(XY)\bar{Z}$ scattering directions, respectively, and the mode assignments remain controversial due to the lack of consensus among different reports. The phonon modes assigned in the earlier reports[7–12] do not obey the selection rules and are therefore incorrect. Let us point out some of the discrepancies in the original polarizing Raman scattering reports, for example, in the cross-polarization, $Z(XY)\bar{Z}$, there should be no A_1 modes, but the polarized Raman scattering study by Fukumura *et al.*[9,10] shows the presence of all A_1 modes with higher intensities (not polarized) compared to the E modes, which is rather unexpected. Haumont *et al.*[8] reported observation of 11 modes in $Z(XX)\bar{Z}$ scattering configuration, but 13 modes in $Z(XY)\bar{Z}$ scattering direction, which violets the Raman selection rules. The Raman scattering experiments by Cazayous *et al.*[11] showed fewer phonon modes in $Z(XX)\bar{Z}$ direction compared to the $Z(XY)\bar{Z}$ direction and all the A_1 modes are not polarized in $Z(XY)\bar{Z}$ scattering direction, which does not follow the selection rules.

Hermet *et al.*[14] have calculated the Raman and infrared active modes in BFO using a first-principles approach based on density-functional theory. The calculated modes are significantly different from the experimental observations, for example, no modes has been obtained below 90 cm^{-1}, contrary to the experimental observation of two Raman actives modes.[9,10,19] We will discuss our results and will explain why all the previous measurements gave incorrect phonon modes in the following sections.

B. Polarized Raman spectroscopy of single-domain $BiFeO_3$ single crystal

Figure 1 shows the polarized Raman spectra of as-grown BFO single-domain single crystal $(100)_{pc}$ cut in $Z(XX)\bar{Z}$, $Z(XY)\bar{Z}$, and $Y(ZX)\bar{Y}$ scattering configurations at 81 K and room temperature. The structural properties of this single crystal have been studied using x-ray diffraction and reported in Refs. 20 and 21. As can be seen from Fig. 1(a), we observed 13 sharp and well-defined peaks in $Z(XX)\bar{Z}$ and only nine peaks in $Z(XY)\bar{Z}$ polarization configurations as theoretically calculated (cf. Table I in Ref. 19). The spectra in $Z(XY)\bar{Z}$ and $Y(ZX)\bar{Y}$ scattering configurations at room temperature [Fig. 1(b)] show only 9E modes, as allowed by Raman selection rules for the rhombohedral structure with $R3c$ symmetry.[19] A multiphonon peak has been observed at around 1250 cm^{-1} [inset Fig. 1(b)] in both the scattering configurations because these peaks are usually depolarized. The A_1 modes were unambiguously isolated from doubly degenerate E modes by comparing the spectra along $Z(XX)\bar{Z}$ scattering configuration with $Z(XY)\bar{Z}$ and $Y(ZX)\bar{Y}$ polarization configurations; the latter ones allow only E modes (cf. Table I in Ref. 19).

In order to differentiate between the transverse optical (TO) and longitudinal optical (LO) phonon modes, we analyzed Raman-active vibrational symmetries and Raman tensor components with different phonon directions.[22] Since the direction of the phonon propagation in $Z(XX)\bar{Z}$, $Z(XY)\bar{Z}$, and $Y(ZX)\bar{Y}$ scattering configurations is perpendicular to the direction of polarization, all of the observed doubly degenerate E modes are purely TO phonon modes.

The A_1 modes observed in $Z(XX)\bar{Z}$ scattering configuration are only LO phonons as the eigenvector is parallel to the Z direction. The A_1 (TO) modes are observed only in $Y(ZZ)\bar{Y}$ scatting configuration (cf. Table I in Ref. 19). The scattering direction of the A_1 (TO) modes in $Y(ZZ)\bar{Y}$ could not extracted very precisely because the scattering along this direction is heavily dominated by Rayleigh scattering. However, in this geometry we observed (Fig. 2) the signature of all the four A_1 modes at about 57, 127, 168, and 212 (very weak) cm^{-1} at 300 K.

In order to get more accurate phonon vibrational energies, we analyzed the spectra using a phonon fitting function. The peaks observed at 74.2, 265.4, 350.4, and 523.1 cm^{-1} were assigned as A_1 modes, contrary to all prior reports on single crystals.[7–12] Haumont *et al.* in Ref. 7 have reported the observation of a total of 11 peaks in BFO single crystal and of

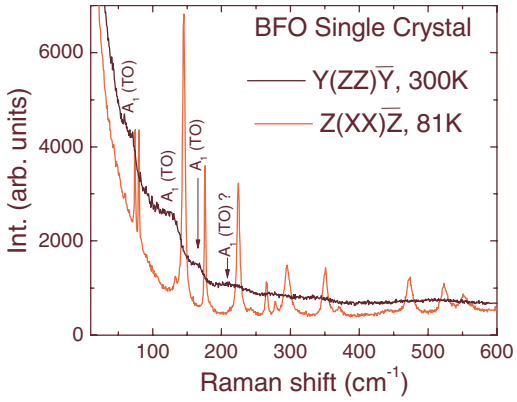

FIG. 2. (Color online) Polarized Raman spectra of single-domain $BiFeO_3$ single crystal in $Y(ZZ)\bar{Y}$ scattering configuration at 300 K. The spectrum along $Z(XX)\bar{Z}$ direction at 81 K is given to distinguish between A_1 (LO) and A_1 (TO) modes.

which four peaks, at 127.1, 141.4, 162.9, and 204.6 cm^{-1} were assigned as A_1 modes.[12] The same authors in their recent paper (in Ref. 8, Fig. 3) reported a total of ten peaks in $Z(XX)\bar{Z}$ and 11 peaks in $Z(XY)\bar{Z}$ configurations but with some new peaks (65 and 255 cm^{-1}), and they assigned six peaks 84, 141, 162, 255, 314, and 530 cm^{-1} as A_1 mode (see results marked superscript [a] in Table I). A significant difference has been observed in comparison with the spectra of the single crystal reported by Haumont *et al.*[8] and of our work on single crystals, for example, we observed the strongest peak at 145 cm^{-1}, in agreement with,[9–11] while they observed the strongest peak around 530 cm^{-1}. In addition, their Raman spectra show a rhombohedral to cubic phase transition around 820 °C,[7,12] which is at variance with the BFO phase diagram in Ref. 23, and its more recent revised versions,[19,24] showing that BFO possesses a noncubic β phase between 820 to 933 °C below the γ phase and the β phase recently was recognized as orthorhombic using high-temperature x-ray diffraction, domain structure, Raman studies,[19] and neutron diffraction.[25] This clearly tells that the single crystal investigated by the authors of Refs. 7, 8, and 12 could have had mixed phases or distortion caused by mechanical polishing.

Although the existence of the strongest peak at around 145 cm^{-1} in our spectra agrees well with the works by Fukumura *et al.*[9,10] and Cazayous *et al.*,[11] some of our assignments are different. Note that the assignment of modes E (LO) and A_1 (TO) in $Z(XX)\bar{Z}$ and $Z(XY)\bar{Z}$ scattering directions by Cazayous *et al.*[11] is forbidden in rhombohedral structure with $R3c$ symmetry and the reported A_1 (TO) mode at 553 cm^{-1} above all A_1 (LO) modes is rather unexpected. The existence of additional and forbidden Raman active modes in Fukumura *et al.*[9,10] and Cazayous *et al.*[11] spectra could be due to the polishing mechanical pressure which might have distorted the direction of polarization as explained in the following section.

C. Polishing effect on single-crystal preparation

Fukumura *et al.*[9,10] used the same growth method as ours[16] for obtaining BFO single crystals and prepared a pseudocubic (111) cut perpendicular to the polar axis for Raman effect studies. Some remarks on the sample preparation may therefore be timely. The single-domain state of our specific crystal was determined by transmission polarized light microscopy, which showed a homogeneous extinction over the whole crystal plate surface with the crossed polarizers aligned along the in-plane pseudocubic [110] directions. In order to maintain the brilliant surface for the Raman measurements, the crystal had not been etched. In such plates with $(100)_{pc}$ surface, the spontaneous polarization is inclined by an angle of ~35° to the surface. It was not possible to determine which of the two mutually perpendicular $(110)_{pc}$ planes was containing the spontaneous polarization vector. This was almost impossible by determining the orientation of the spontaneous birefringence with a compensator, due to the "giant" spontaneous birefringence of rhombohedral $BiFeO_3$,[26] combined with a large thickness (~30 μm), not permitting to identify the addition or substraction position due to too high order in the Michel-Lévy interference color chart. Fukumura *et al.*[9,10] reported that their pseudocubic as-grown (100) and polished (111) surfaces were not in an entirely single-domain state. Therefore they had to conceive a method of line illumination with a resolution of 2.5 μm, in

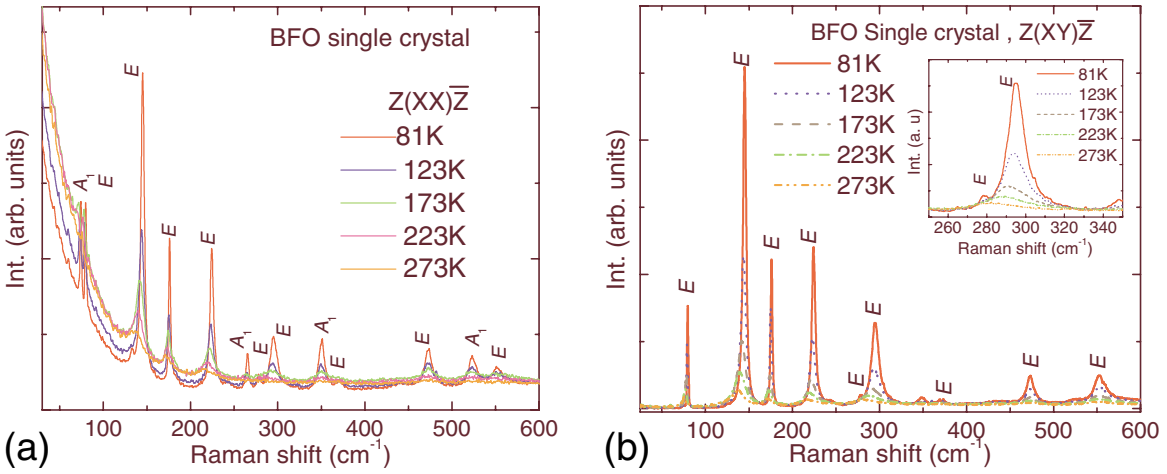

FIG. 3. (Color online) Temperature-dependent polarized Raman spectra of as-grown single-domain $BiFeO_3$ single crystal from 81–273 K at different scattering configurations; (a) along $Z(XX)\bar{Z}$ and (b) $Z(XY)\bar{Z}$.

TABLE I. Comparison of Raman active modes and symmetry assignment of $BiFeO_3$ single crystal: earlier reported results with the present work.

Earlier reports								Present work	
Frequency[a] (cm^{-1})	Symmetry[a] assignment	Frequency[b] (cm^{-1})	Symmetry[b] assignment	Frequency[c] (cm^{-1})	Symmetry[c] assignment	Frequency[d] (cm^{-1})	Symmetry[d] assignment	Frequency (cm^{-1})	Symmetry assignment
56		56.1	E					57.0	A_1 (TO)
65				77	E	75	E (TO)	74.2	A_1 (LO)
84	A_1	84.1	E			81	E (LO)	79.6	E (TO)
95		95.3	E						
127		127.1	A_1	136	E	132	E (TO)	127.0	A_1 (TO)
141	A_1	141.4	A_1	147	A_1	145	A_1 (LO)	145.0	E (TO)
162	A_1	162.9	A_1					168.0	A_1 (TO)
162	A_1	162.9	A_1	176	A_1	175.5	A_1 (LO)	175.9	E (TO)
205		204.6	A_1					212.0	A_1 (TO)
				227	A_1	222.7	A_1 (LO)	224.2	E (TO)
255	A_1								
		261.3	E	265	E	263	E (TO)	265.4	A_1 (LO)
				279	E	276	E (TO)	277.7	E (TO)
314	A_1	316.6	E			295	E (TO)	295.2	E (TO)
				351	E	348	E (TO)	350.4	A_1 (LO)
		383.6	E	375	E	370	E (TO)	371.5	E (TO)
				437	E	441	E (TO)		
				473	E	471	A_1 (LO)	473.0	E (TO)
				490	A_1				
531	A_1	530.9	E	525	E	523	E (TO)	523.1	A_1 (LO)
						550	A_1 (TO)	553.0	E (TO)

[a]Reference 8.
[b]References 7 and 12.
[c]References 9 and 10.
[d]Reference 11.

order to penetrate into individual domains. Their polydomain state was probably caused by mechanical manipulations, because the ferroelastic domains of $BiFeO_3$ can be easily moved by applying stress, whereas the as-grown crystals proved always to be both ferroelectric and ferroelastic single domains because it was as grown below the α/β-phase transition temperature.[16,20] In preparing a polished pseudocubic (111) cut perpendicular to the polar axis, a further difficulty resides in the fact that the [111] space diagonal of the pseudocubic rhombohedral cell is longer than the three other space diagonals. Therefore, for a sample with the polar axis perpendicular to the plate, the polishing pressure leads to a switching of the correctly oriented domain into one or all of the three domain states having the spontaneous polarization inclined to the surface. This polishing effect was noted on a transparent $(111)_{pc}$ wafer both by means of conoscopy and orthoscopy (H. Schmid, unpublished, 1986). The black cross obtained with crossed polars of the uniaxial conoscopic figure (see Fig. 7b in Ref. 19) did not stay immobile by rotating the crystal by 360°, but opened very slightly at 60° (120)° intervals, mimicking optically biaxial domains. Subsequent orthoscopic observation revealed in fact a very thin layer of polishing-stress-induced domains with inclined rhombohedral principal axis. Thanks to the "giant" spontaneous birefringence of the rhombohedral phase.[26] These domains have been identified with faint gray contrast, corresponding to a path differences of the first-order Michel-Lévy interference color chart and permitting an estimation of the layer thickness to about 150–200 nm (!!). The interpretation of Raman spectra and other surface-sensitive measurements of $BiFeO_3$ requires therefore a careful examination of the ferroelastic domain state close to the surface.

Lebeugle *et al.*[27] have shown by neutron scattering, that a ferroelectric single domain in the antiferromagnetic phase is characterized by a cycloidal modulation vector along a single pseudocubic ⟨110⟩ direction. This means that the symmetry is lowered to an average monoclinic structure. Similar results have been obtained by Lee *et al.*,[28] but the decreased symmetry is not pointed out explicitly. The situation has been explained in detail by Schmid.[29] Although it is probable that the ferroelectric single domain used in this work was also magnetically a single domain, i.e., with a cycloidal modulation vector along a single pseudocubic ⟨110⟩ direction (parallel to monoclinic principal axis), we have no prove since the sample was not tested by neutron diffraction.

The fact that Raman spectra and selection rules may be less compatible with theory in single crystals than in films

may seem very surprising, but the reason is that single crystals are often mechanically polished. As first shown by Scott[30] this produces large inhomogeneous strain. Inhomogeneous strain is far more effective in breaking selection rules than is the homogeneous strain that may be present in thin films from substrate lattice mismatch; in particular, it can permit odd-parity phonon lines to show up in the Raman spectra of centric crystals.

Opaque materials such as $BiFeO_3$ are usually studied using micro-Raman spectroscopy. Such apparatus requires a 180° backscattering geometry. As shown by Scott and Porto[31] these geometries cannot differentiate among certain phonon symmetries in twinned crystals; single-domain specimens, as in the present work, are required. This particular Raman selection-rule violation was first interpreted quantitatively by Scott[30] in terms of inhomogeneous strain born and brought up by mechanical polishing of scheelite. Note, in particular, that it cannot arise from homogeneous shear strain.

A comparison of all prior reports with the present work has been made in Table I. Our assignments are based on the polarized Raman spectra taken along different scattering orientations as reported in Fig. 1.

D. Low-temperature Raman spectroscopy of single-domain $BiFeO_3$

Figure 3 shows the temperature dependence (from 81 K to room temperature) of polarized Raman spectra of single-domain $BiFeO_3$ in $Z(XX)\bar{Z}$ and $Z(XY)\bar{Z}$ scattering configurations. The spectra were recorded during controlled warming and the temperature was stabilized for 10 min after reaching the set temperature with 10 min spectrum acquisition time. No significant change in the vibrational phonon frequencies has been observed with increasing temperature indicating that the $R3c$ symmetry remains unchanged. However, a very slight shift in the phonon frequency bands toward lower wave number and the associated broadening have been observed, which can be explained by thermal expansion and disorder. Several second-order phonon vibrations (not shown) at around 605 (very weak), 720, 807, 930, 948, 1091, and 1149 cm^{-1} have been observed in $Z(XX)\bar{Z}$ scattering direction and almost the same number were observed in the $Z(XY)\bar{Z}$ scattering configuration, which can be explained by the fact that almost all the second-order peaks are mostly (>80%) depolarized.

E. Raman spectroscopy of $BiFeO_3$ single crystal and thin film: A comparative study

In order to understand the crystallographic correlation between BFO single crystal and thin film, we investigated 300-nm-thick BFO films grown on SRO/STO(100) substrates. The presence of sharp and distinct peaks on the XRD pattern (Fig. 4) of the BFO film confirms single phase and c-axis (pseudocubic ⟨001⟩ direction, perpendicular to the substrate) orientation. The c-axis length of the BFO films was calculated and found to be 3.95 Å, which is very close to the reported c-axis length (c=3.997 Å).[6] Comparing the full width at half maxima of (003) peak (Fig. 4) with the reported

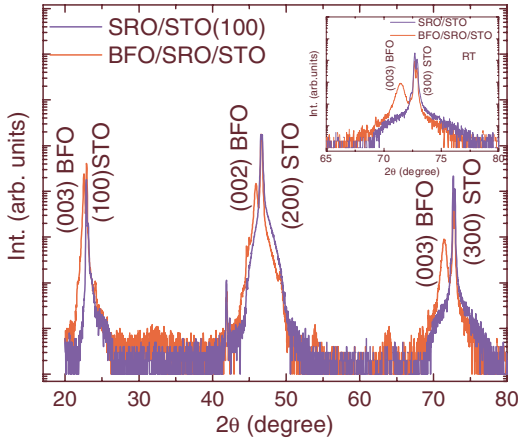

FIG. 4. (Color online) XRD pattern of $BiFeO_3$ thin film on STO(100) substrate with SRO (25 nm) bottom electrode. SRO peaks are not seen, as they are very weak and lie in the proximity of STO peaks. Inset shows (003) peak of $BiFeO_3$ thin film.

results in Ref. 1, it was found that our films are highly crystalline in nature.

The polarized Raman spectra (Fig. 5) for 300-nm-thick (001)BFO thin film on the (100)STO substrate at 81 K in the parallel $Z(XX)\bar{Z}$ and perpendicular $Z(XY)\bar{Z}$ scattering configurations reveal peaks at 74.2, 79.3, 147.0, 176.1, 224.0, 363.6, 273.3, 294.1, 348.7, 374.3, 411.0, 472.8, 521.7, and 547.7 (very weak), with few broad second-order peaks (not shown) at 610, 710, 806, 926, 948, 1092, and 1152 cm^{-1}. All of these peaks are due to the BFO normal modes of vibrations and none of them is arising from the substrate (cf. Fig. 2 in Ref. 19). We verified our results using target materials, single crystal, and also growing (001)BFO films on different substrates.

The existence of 13 (excluding one weak peak) sharp and well-defined peaks [Fig. 5(a)] in both the $Z(XX)\bar{Z}$ and $Z(XY)\bar{Z}$ polarization configurations of (001)BFO thin film does not follow the Raman selection rules for the tetragonal or rhombohedral symmetry (cf. Table I in Ref. 19) as reported earlier[1–5] rather it confirms the monoclinic structure. This observation agrees with the very recent report of monoclinic structure for the (001) BFO films grown on STO substrates by Xu *et al.*[6] studied via synchrotron radiation. We also investigated (001)BFO thin films grown using different deposition techniques (PLD) and chemical solution deposition on different single crystal and textured substrates and we found that films show monoclinic structure at room temperature down to 50 nm thick. The comparison of single crystal [Fig. 3(a)] and thin-film spectra [Fig. 5(a)] at 81 K in $Z(XX)\bar{Z}$ and $Z(XY)\bar{Z}$ scattering configurations clearly shows that the thin film has a different crystallographic symmetry compared to the single crystal.

Figure 5(b) shows the comparison of unpolarized Raman spectra of single-domain BFO single crystal and (001)BFO thin film. As can be seen, thin film shows only one additional first-order Raman mode (indicated with arrow at 411.0 cm^{-1}), except that all other signatures of the single crystal including small leakage component because the crystallographic axes are not exactly orthogonal (α=89.5°), have been observed in thin film reflecting the good quality. There

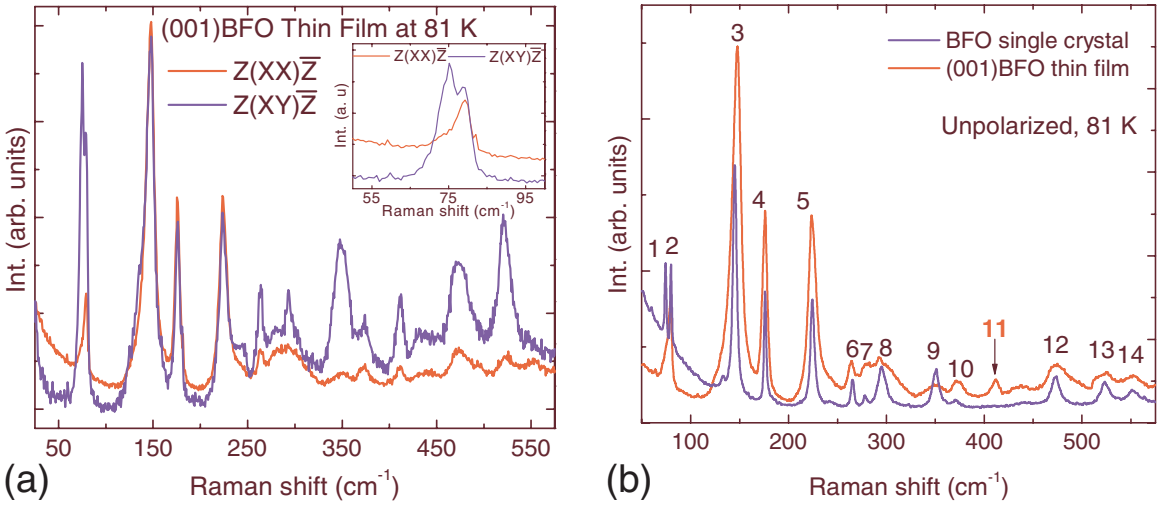

FIG. 5. (Color online) (a) Polarized Raman spectra of (001)$BiFeO_3$ thin film on SRO/STO in Z(XX)$\bar{Z}$ and Z(XY)$\bar{Z}$ scattering configurations at 81 K. The inset shows the magnification 50–100 cm^{-1}. (b) Comparison of unpolarized Raman spectra of as-grown single-domain BFO single crystal with (001)BFO thin film at 81 K.

are two nominal possibilities for considering unique axis in the monoclinic structure. When c axis consider as the unique axis $13A'$ modes are allowed in both the Z(XX)$\bar{Z}$ and Z(XY)$\bar{Z}$ scattering configurations. Thus this geometry does not permit strict determination of symmetry. However, if the b axis is considered (more correctly) as the unique axis the Raman tensors for point group (C_s) can be written as[22]

$$\begin{pmatrix} a & & d \\ & b & \\ d & & c \end{pmatrix} \quad \begin{pmatrix} & e & \\ e & & f \\ & f & \end{pmatrix}$$

$$A'(X,Z) \quad A''(Y).$$

This implies $13A'$ and $14A''$ modes are allowed in Z(XX)$\bar{Z}$ and Z(XY)$\bar{Z}$ scattering configurations, respectively.

Since there is uncertainty in assigning the polar axis in monoclinic phases, the transverse and longitudinal optical phonons cannot be assigned unambiguously. This would required geometries different from backscattering, as explained in Ref. 31. Such geometries are generally impossible for opaque samples or for micro-Raman setups. The polar axis parallel to the Z axis (c axis as unique axis) allows only A' (TO) modes in both Z(XX)$\bar{Z}$ and Z(XY)$\bar{Z}$ scattering configurations, while the unique axis parallel to the Y axis (b axis as unique axis) allows A' (TO) and A' (LO) modes in Z(XX)$\bar{Z}$ scattering configuration and 14 A'' (TO) modes in Z(XY)$\bar{Z}$ scattering configurations. No significant splitting has been observed between A' (TO) and A' (LO) phonons in thin films, as in single crystals. As the spectra along Y(ZZ)$\bar{Y}$ and Y(ZX)$\bar{Y}$ were heavily dominated by the scattering from the STO substrate, the contribution from the BFO film could not be separated. More detailed studies on dynamics of phonon modes in BFO(001) films by Raman spectroscopy is given in Ref. 32. Since the earlier assignment of Raman active modes in BFO(001) thin films were made by incorrectly suggesting tetragonal or rhombohedral structure,[2,5] the comparison of old thin-film assignment with the present result is irrelevant.

The higher dimensional incommensurate magnetic space group in BFO single crystal, so far not known, should not allow the linear magnetoelectric effect. However, it does allow the quadratic magnetoelectric effect, as has been demonstrated on single crystals.[33] Since the film has different symmetry from bulk, the linear magnetoelectric effect might be possible in thin film, provided the incommensurability would be suppressed. The observation of such a linear magnetoelectric effect has been claimed in Ref. 1 for a ferromagnetic film of BFO. However, a careful magnetoelectric coupling experiment and neutron diffraction of (001)BFO films would be interesting to verify the potential suppression of cycloidal spin structure in epitaxial thin film.

IV. CONCLUSION

In conclusion, the polarized Raman spectra of single-domain BFO single crystal in different scattering configurations clearly follow the rhombohedral symmetry with $R3c$ space group. All the phonon vibrations have been assigned unequivocally contrary to all prior reports. Epitaxial (001)BFO films grown on (100)STO substrates using PLD showed that the films are c axis oriented with high degree of crystallinity. The room-temperature-polarized Raman scattering of (001)BFO films showed monoclinic symmetry, in agreement with the synchrotron studies.

The impact of this work on the general application of $BiFeO_3/SrTiO_3$ heterojunction films for magnetoelectric devices is that the magnetoelectric tensor at room temperature must be that for monoclinic crystal class, contrary to that inferred in Refs. 1–4 and 33. Moreover, in nonepitaxial films monoclinic domain walls may therefore be expected and could complicate performance.

ACKNOWLEDGMENTS

We thank T. Pradhan for helpful discussions. The help of W. Perez and S. R. Das for polarization measurement and target preparation is gratefully acknowledged. The authors would like to acknowledge financial support from DOE under Grant No. DE-FG02-08ER46526. R.P. thanks Institute for Functional Nanomaterial (IFN), UPR for financial support. The $BiFeO_3$ single-domain crystal was grown in 1992, thanks to a Swiss NSF grant.

[1] J. Wang, J. B. Neaton, H. Zheng, V. Nagarajan, S. B. Ogale, B. Liu, D. Viehland, V. Vaithyanathan, D. G. Schlom, U. V. Waghmare, N. A. Spaldin, K. M. Rabe, M. Wuttig, and R. Ramesh, Science **299**, 1719 (2003).

[2] M. K. Singh, S. Ryu, and H. M. Jang, Phys. Rev. B **72**, 132101 (2005).

[3] R. R. Das, D. M. Kim, S. H. Baek, C. B. Eom, F. Zavaliche, S. Y. Yang, R. Ramesh, Y. B. Chen, X. Q. Pan, X. Ke, M. S. Rzchowski, and S. K. Streiffer, Appl. Phys. Lett. **88**, 242904 (2006).

[4] X. Qi, J. Dho, R. Tomov, M. G. Blamire, and J. L. MacManus-Driscoll, Appl. Phys. Lett. **86**, 062903 (2005).

[5] Y. Yang, J. Y. Sun, K. Zhu, Y. L. Liu, and L. Wan, J. Appl. Phys. **103**, 093532 (2008).

[6] G. Xu, H. Hiraka, G. Shirane, J. Li, J. Wang, and D. Viehland, Appl. Phys. Lett. **86**, 182905 (2005).

[7] R. Haumont, J. Kreisel, P. Bouvier, and F. Hippert, Phys. Rev. B **73**, 132101 (2006).

[8] R. Haumont, J. Kreisel, and P. Bouvier, Phase Transitions **79**, 1043 (2006).

[9] H. Fukumura, S. Matsui, H. Harima, T. Takahashi, T. Itoh, K. Kisoda, M. Tamada, Y. Noguchi, and M. Miyayama, J. Phys.: Condens. Matter **19**, 365224 (2007).

[10] H. Fukumura, H. Harima, K. Kisoda, M. Tamada, Y. Noguchi, and M. Miyayama, J. Magn. Magn. Mater. **310**, e367 (2007).

[11] M. Cazayous, D. Malka, D. Lebeugle, and D. Colson, Appl. Phys. Lett. **91**, 071910 (2007).

[12] S. Kamba, D. Nuzhnyy, M. Savinov, J. Šebek, J. Petzelt, J. Prokleška, R. Haumont, and J. Kreisel, Phys. Rev. B **75**, 024403 (2007).

[13] H. Bea, M. Bibes, S. Petit, J. Kreisel, and A. Barthelemy, Philos. Mag. Lett. **87**, 165 (2007).

[14] P. Hermet, M. Goffinet, J. Kreisel, and Ph. Ghosez, Phys. Rev. B **75**, 220102(R) (2007).

[15] T. Pradhan, Phys. Scr. **45**, 86 (1992).

[16] F. Kubel and H. Schmid, J. Cryst. Growth **129**, 515 (1993) (erratum). In Fig. 11 the bold-type arrows (∥ cubic ⟨111⟩ directions) should not form 45° with the horizontal, but 35.26°.

[17] A. M. Glazer, Acta Crystallogr. B **28**, 3384 (1972).

[18] C. Ederer and N. A. Spaldin, Phys. Rev. B **71**, 060401(R) (2005).

[19] R. Palai, R. S. Katiyar, H. Schmid, P. Tissot, S. J. Clark, J. Robertson, S. A. T. Redfern, G. Catalan, and J. F. Scott, Phys. Rev. B **77**, 014110 (2008).

[20] F. Kubel, Z. Kristallogr. **210**, 5 (1995).

[21] F. Kubel and H. Schmid, Acta Crystallogr. B **46**, 698 (1990).

[22] R. Loudon, Adv. Phys. **13**, 423 (1964).

[23] E. I. Speranskaya, V. M. Skorikov, E. Y. Rode, and V. A. Terekhova, Bull. Acad. Sci. USSR, Div. Chem. Sci. **14**, 873 (1965).

[24] C. Tabares-Muñoz, Ph.D. thesis, University of Geneva, 1986.

[25] D. C. Arnold, K. S. Knight, F. D. Morrison, and P. Lightfoot, Phys. Rev. Lett. **102**, 027602 (2009).

[26] J.-P. Rivera and H. Schmid, Ferroelectrics **204**, 23 (1997).

[27] D. Lebeugle, D. Colson, A. Forget, M. Viret, A. M. Bataille, and A. Gukasov, Phys. Rev. Lett. **100**, 227602 (2008).

[28] S. Lee, T. Choi, W. Ratcliff II, R. Erwin, S.-W. Cheong, and V. Kiryukhin, Phys. Rev. B **78**, 100101(R) (2008).

[29] H. Schmid, J. Phys.: Condens. Matter **20**, 434201 (2008).

[30] J. F. Scott, J. Chem. Phys. **48**, 874 (1968); **49**, 98 (1968).

[31] J. F. Scott and S. P. S Porto, Phys. Rev. **161**, 903 (1967).

[32] R. Palai, J. F. Scott, and R. S. Katiyar, Phys. Rev. B **81**, 024115 (2010).

[33] C. Tabares-Munoz, J. P. Rivera, A. Bezinges, A. Monnier, and H. Schmid, Jpn. J. Appl. Phys., Suppl. 24-2, **24**, 1051 (1985).